Original Article

An inertial measurement unit tracking system for body movement in comparison with optical tracking

Rui Li[1] iD **, Barclay Jumet**[1,2]**, Hongliang Ren**[3]**, WenZhan Song**[1] **and Zion Tsz Ho Tse**[1,4] iD

Abstract

The recent advancement of motion tracking technology offers better treatment tools for conditions, such as movement disorders, as the outcome of the rehabilitation could be quantitatively defined. The accurate and fast angular information output of the inertial measurement unit tracking systems enables the collection of accurate kinematic data for clinical assessment. This article presents a study of a low-cost microelectromechanical system inertial measurement unit-based tracking system in comparison with the conventional optical tracking system. The system consists of seven microelectromechanical system inertial measurement units, which could be mounted on the lower limbs of the subjects. For the feasibility test, 10 human participants were instructed to perform three different motions: walking, running, and fencing lunges when wearing specially designed sleeves. The subjects' lower body movements were tracked using our inertial measurement unit-based system and compared with the gold standard—the NDI Polaris Vega optical tracking system. The results of the angular comparison between the inertial measurement unit and the NDI Polaris Vega optical tracking system were as follows: the average cross-correlation value was 0.85, the mean difference of joint angles was 2.00°, and the standard deviation of joint angles was ± 2.65°. The developed microelectromechanical system–based tracking system provides an alternative low-cost solution to track joint movement. Moreover, it is able to operate on an Android platform and could potentially be used to assist outdoor or home-based rehabilitation.

Introduction

Motion tracking has received extensive attention since the 1990s.[1–4] Several techniques allow for motion reconstruction based on different information sources. As one of its primary applications, motion tracking has been used for monitoring rehabilitation progress of movement disorders.[5] Movement disorders refer to a group of conditions that are related to the nervous system and cause unusual body movements. Common movement disorders include Huntington's disease[6] and Parkinson's disease.[7,8] As an example, Parkinson's disease is a chronic neurodegenerative disorder that has affected 1 million people in the United States and 5 million people worldwide.[9] There is a specific type of rehabilitation, called neurorehabilitation, aimed at treating conditions, such as movement disorders, where patients repetitively move their limbs so that the functional patterns can be produced. The motion tracking could

provide feedback to the patients as well as the therapist in real time.

One of the biggest challenges in motion tracking is to obtain an accurate estimation with non-invasive sensors within a confined workspace. A mainstream solution is to use the optical tracking system (OTS). The NDI Polaris Vega® system, for example, delivers a

[1]School of Electrical & Computer Engineering, University of Georgia, Athens, GA, USA
[2]Department of Mechanical Engineering, University of Alabama, Tuscaloosa, AL, USA
[3]Department of Biomedical Engineering, National University of Singapore, Singapore
[4]Department of Electronic Engineering, The University of York, York, UK

Corresponding author:
Zion Tsz Ho Tse, Department of Electronic Engineering, The University of York, Heslington, York YO10 5DD, UK.
Email: zion.tse@york.ac.uk

tracking accuracy of 0.12 mm root mean square (RMS) and 95% confidence interval accuracy to 0.2 mm at a measurement rate of 60–250 Hz. The main disadvantage of the OTS is the requirement for a clear line-of-sight between the patient, the instrument trackers, and the optical cameras.

Recently, a type of inertial measurement unit (IMU) called microelectromechanical system (MEMS) IMUs has given a new surge to motion tracking research.[10–13] These systems are cost-effective for providing accurate, non-invasive, and portable motion measurements. The primary point of interest in these systems is that they can overcome the limitations of optical systems and mechanical trackers. In one of the early studies, Ren and Kazanzides[14] used raw data from a class of miniaturized IMU—integrated system of the magnetic field, angular rate, and gravity (MARG)—to estimate the orientation of a surgical instrument; this again demonstrated the IMU's ability to track movement.

Much research work has been published based on motion tracking using different types of IMUs, such as Xsens,[15] Opal,[16] and Noraxon.[17] In the area of joint movement, Kobashi et al.[18] presented a method to measure the knee joint angle using MARG; however, the sensor is not cost-effective for the users. Müller et al.[19] have developed a model to measure elbow angles, which introduced a concept of self-calibration. Mundt et al.[20] published a comprehensive assessment of using both IMUs and optoelectronic systems for 3D joint angles measurement. However, the tasks were limited, for example, walking and stair-step exercises. The system developed in this article was different from the existing ones as it could operate on an Android smartphone environment, as explained in the author's previous publication.[21] The smartphone application provides real-time movement tracking so that the users can carry out repetitive and straightforward rehabilitation exercises in home or outdoor environment. Furthermore, the kinematic data collected by the application could be uploaded and shared with the physical therapists for future treatment planning.

In this study, the tracking accuracy of our MEMS IMU-based tracking system was quantitatively assessed, and the results were compared with the NDI system (NDI, Ontario, Canada) for three different typical OTS tasks: walking, running, and fencing lunges. The NDI was used because it is highly accurate and easy to set up. One limitation of the study is that only 2D body movements were studied. This is because our focus was on the angular variations of the hip, knee, and ankle only within the sagittal plane. Therefore, we believe that 2D kinematic analysis is sufficient in this study. However, in the future, a 3D kinematic analysis may be carried out as it could help reveal more movement details.

Table 1 highlights the differences between our system and the existing ones. First, the system offers a low-cost solution compared to the existing systems. Second, the MEMS IMU system can output acceleration reading in real time since a built-in accelerometer was included. In contrast, the systems like the OTS can only calculate acceleration based on the trajectories of reflective markers. With the acceleration information, the users would benefit from knowing how fast they can perform an exercise. Moreover, the MEMS IMU system was wireless and wearable by the test subject, providing a high degree of flexibility required for exercise, whereas the OTS has field-of-view and line-of-sight problems. When using the OTS, tracking errors or phantom points are generated when the reflective markers are blocked or not positioned correctly. However, some limitations of MEMS IMU systems are that the IMU can suffer from drift due to instrumentation biases, and more affordable IMUs are prone to noisy data and a lack of precision relative to other tracking systems.

Table 1. Comparison of functionality between our system and the existing ones.

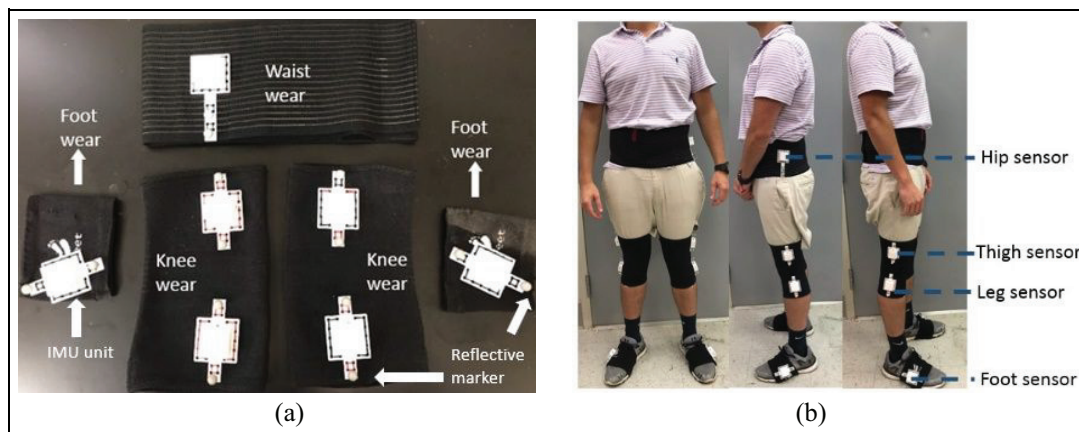|	Robotics system	VR rehabilitation	OTS system	Our system
Low-cost solution	No, price range: US$18,000–US$40,000[22,23]	No, price range: US$1400–US$2000[24,25]	No, price range (passive system): US$150,000–US$250,000[26]	Yes, the IMU modules cost US$280, 3D printing material US$10, and flexible bands US$20. The total cost is US$310.
Easy-to-use	No	Yes	No	Yes
Outdoor use	No	No	No	Yes
Exercise range limitation	No	Yes, near a station (desktop, laptop)[27]	Yes, within the coverage area of the camera system, NDI tracking range: 2400 mm[28]	No
Portable	No	No	No	Yes
Data logging	Yes	Yes	Yes	Yes
Data sharing	No	No	No	Yes
Acceleration info	No	No	No	Yes

Figure 1. (a) The overview of the tracking system with reflective markers and (b) mounting locations on the hip, knees, and ankles of end users. The IMU modules were placed on the outer surface of the hip, knees, and ankles.

Table 2. Head-to-head comparison between the IMU and the NDI optical tracking system.

	Specification of the IMU system	NDI
Dimensions	For individual sensors: 37(L) $\times$ 34(W) $\times$ 19.7(H) mm	591(L) $\times$ 103(W) $\times$ 106(H) mm
Components	Reed switch	Near-infrared (IR) light
	12(L) $\times$ 2.9(W) $\times$ 1.4(H) mm	
	Acceleration: $\pm$ 16 g	IR sensor, sampling rate: 60 Hz
	Angular speed measurement: $\pm$ 2000°/s	
	Angular measurement: $\pm$ 180°	
	Accuracy of angular reading: 0.01°	
	Sampling rate: 50 Hz	
	Communicate to smartphone	Reflective markers
	Valid range: 10 m	

Materials and methods

The purpose of this study was to develop a new MEMS IMU-based angular tracking system that could be integrated with an Android platform to monitor human movement. Figure 1 shows the tracking system as well as the mounting locations of the sensors.

IMU system design

The system was designed to track the whole body posture with seven mountable IMU sensors. Each sensor outputs the movement angle of different parts of the leg. A therapist may evaluate the performance of the patient based on the recorded angular data. The specifications of the tracking system are shown in Table 2.

Figure 2 shows the IMU sensor's internal components and how the IMU is integrated with the optical markers and the overall set up design.

Participants

In total, 10 healthy human volunteers (sex: M/F, age: > 18 years, body mass: 75 $\pm$ 10 kg, height: 170 $\pm$ 10 cm) were recruited in this study. The study was carried out with approval from the University of Georgia Institutional Review Board. All participants were pre-screened by the eligibility assessment. The inclusion criteria for the study were healthy adults who exercise regularly. The exclusion criteria were the knee/ankle problems, non-healing wounds, ulceration, gangrene, pain with exercise, pain at rest, claudication, arterial grafts or clots, walking impairments, or extremity pain from other causes, and cardiovascular disease. The participants gave informed consent to their inclusion in the study as required, and the work adhered to the Declaration of Helsinki. Each participant performed three different motions: walking, jogging, and fencing lunge. The overall exercise time was about 25 min, including preparation.

Planned exercise

In this study, three different exercises were planned: walking, running, and fencing lunge. For the walking task, the average walking speed is 3.2 km/h. For the jogging task, the average running speed is 5.1 km/h. For the fencing lunge task, the participant was instructed to
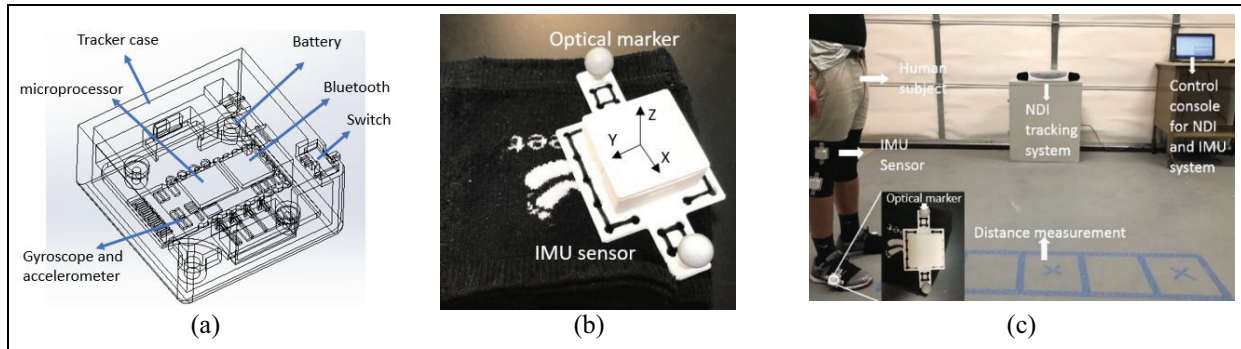
Figure 2. (a) The interior structure of the IMU sensor, which has a gyroscope and an accelerometer, a microprocessor, a battery, a Bluetooth module, and a switch. All the components were placed in a 3D-printed case, (b) the coordinate system of the IMU sensor, and (c) the experimental set up for human trials. The blue lines on the floor are the measuring distance, and the IMU sensor was mounted on human participants using flexible bands. The NDI equipment was set on the table at a detectable distance to the participants. The control console was placed nearby for data recording.
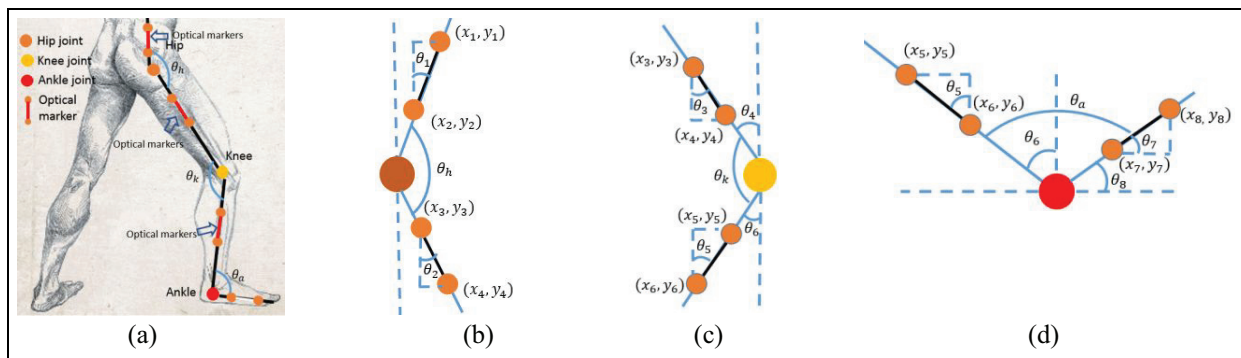

Figure 3. (a) NDI lower-limb kinematic analysis and NDI segmented kinematics analysis for each NDI marker on the (b) hip, (c) knee, and (d) ankle. Each segment was defined based on the joint region between the waist and the thigh, the thigh and the leg, the leg and the foot, respectively.

perform one lunge motion. The average speed is 4.8 km/h. Both the IMU and NDI data were collected in the same trials.

Application of NDI

The experiment was set at a distance of 1.5 m from the NDI, and the walking distance was set at 2 m for markers to remain in the detectable range. NDI claims to have a volumetric accuracy of 0.12 mm RMS. However, three main challenges when using the NDI are the blockage of optical markers during exercise, the alignment between the optical markers, and the positioning of optical markers relating to the IMU sensors and tracking range of NDI. In addition, the position of the optical markers (NDI) and IMU sensors for each wearable sleeve had to be on the same plane and centerline so that there would be the same pivot point for the calculation of angles. The calculations use a two-line angle determination as opposed to a three-vertex angle determination (Figure 3). Each limb segment had a sleeve where the IMU was sewn into place following the longitudinal axis of the pertinent segment. Two

NDI markers were placed around each IMU, one superior and one inferior to the IMU along the same longitudinal axis (Figure 1). The two markers would then be able to be two points on a line that imitated the segment's position and motion. This line could then be analyzed relative to other limb segment lines for determining the angle between two segments and, thus, the joint angle. This allowed us to disregard the interpreted position of the joint determined by the NDI that would have resulted from placing one marker per segment with a median marker placed on each joint. This was preferred because joints are complex anatomical objects that do not move as consistently as limb segments due to the internal structure, causing the outer skin to move and stretch in all directions, which would make joint angle calculations less accurate.

Furthermore, the two-line determination allows for consistent data collection and interpretation across both data sets since IMUs also use a two-line determination. The body movement for a full exercise cycle was studied to ensure the kinematic equations were generalized and could be applied to different scenarios (walking, jogging, and fencing lunges). The movement

cycle of a fencing lunge has five significant steps: (1) on-guard position, (2) lifting of the lead leg, (3) forward flying phase of the lead leg and push-off with the trail leg, (4) landing of the lead foot, and (5) final lunge position.

Design consideration of MEMS IMU-based angular tracking system

Three main design criteria were addressed in this study. The first criterion was the orientation of the IMU. Since the IMUs commonly have a drift problem on the yaw angles, the orientation of the IMU was set to be vertical (Figure 2(b)). Therefore, the reading of yaw angles from the Z-axis did not need to be used as the experiment consisted of two-dimensional motion analysis. The pitch and roll angles were calibrated with the gravity vector, and therefore drifting was not an issue. The second criterion was the mounting method and the positioning of the IMU. During the jogging and fencing lunge exercises, the IMU module could be easily detached from the body. The solution was to use a stretchable waist, thigh, and foot sleeves with the IMU sensors sewn on the surface. With this design, not only could the sensors be mounted more securely and adequately on the designated position but less time was also required for the test preparation.

In addition, the sleeves were more comfortable and were able to fit many different body types with no adjustment. This proper fitting also disallowed significant relative movement of the components during and in between exercises. The final criterion was the derivation of joint angles from the IMU data. As mentioned for the NDI, the pivot point was defined as the intersection between two straight lines projected from the two longitudinal markers on each sleeve, and each straight line was defined by the physical position of the IMU sensors as the markers were placed equidistant from the IMU. By centering the IMU between the two markers, this allowed for the NDI and IMU local coordinate systems of each limb segment to have similar origins to facilitate data analysis after the experiment better.

Kinematics analysis

The kinematic analysis has two separate parts. The first part is to analyze and derive one set of equations describing the joint angles using the positional markers (NDI). The second part is to derive another set of equations describing the joint angles using the orientation of the IMU sensors. Table 3 shows all the symbols used for kinematic analysis. For angle θ'_{ny} and θ'_{nx}, the measurements were taken directly from the gyroscope module inside the IMU and displayed on the user interface of the PC software.

Kinematics analysis for NDI system. Figure 3 shows the detailed kinematics analysis for the NDI system; the

Table 3. Variable definitions for kinematic equations.

Variable	Definition
$\theta_h, \theta_k, \theta_a$	Hip, knee, and ankle joint angle for the NDI
θ_n	Segment angles for the NDI
x_n, y_n	X and Y coordinates from the NDI system for positional markers
$\theta'_h, \theta'_k, \theta'_a$	Hip, knee, and ankle joint angle for the IMU
θ'_n	Segment angles for the IMU
$\theta'_{ny}, \theta'_{nx}$	Angular readings of pitch and roll from the IMU

optical markers have been placed on the waist, thigh, and leg sections of the human body. Three segments were used to construct the model: the waist, knee, and ankle (Figure 3(b)–(c)). The hip segment was defined as the joint region between the waist and thigh sections of the human body. The knee segment was defined as the joint region between the thigh and leg sections of the human body; the ankle segment was defined as the joint region between the thigh and foot sections of the human body. Equations (1)–(9) in the Supplemental Appendix show how to calculate the hip, knee, and ankle angles based on the two pairs of reflective markers.

Kinematics analysis for MEMS IMU-based angular tracking system. Figure 4 shows the detailed kinematics analysis for the IMU system. Equations (10)–(18) in the Supplemental Appendix show how to calculate the hip, knee, and ankle angles based on the two IMUs.

Pretest calibration

The IMUs were calibrated through a method named static test to reduce the tracking errors of angular measurement. In detail, each IMU module was placed on a flat surface and rotated on three axes, one at a time. The axis alignment between the IMU module and the surface was calibrated. After the calibration, another test was carried out on an inclined surface with an adjustable angle. The angular reading from the IMUs was then compared to a protractor, which was used as a reference. If the angular difference between the IMUs and protractor is less than 0.05°, the IMUs were ready to use in the exercises.

Statistical tool

In this study, the cross-correlation method was used to assess the similarity between two sets of data—the IMU and the NDI. As the sampling rate of two systems is different, in order to do cross-correlation, the raw data of each system were first pre-processed and ensured that the time stamp was consistent for both data sets. The cross-correlation method allows for an angle-to-angle
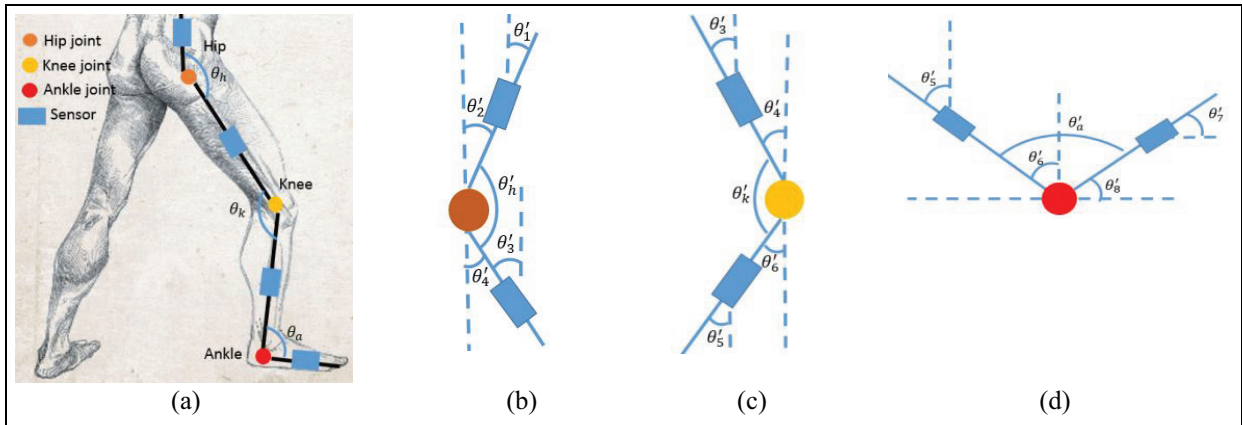
Figure 4. (a) NDI lower-limb kinematic analysis and NDI segmented kinematics analysis for each NDI marker on the (b) hip, (c) knee, and (d) ankle.
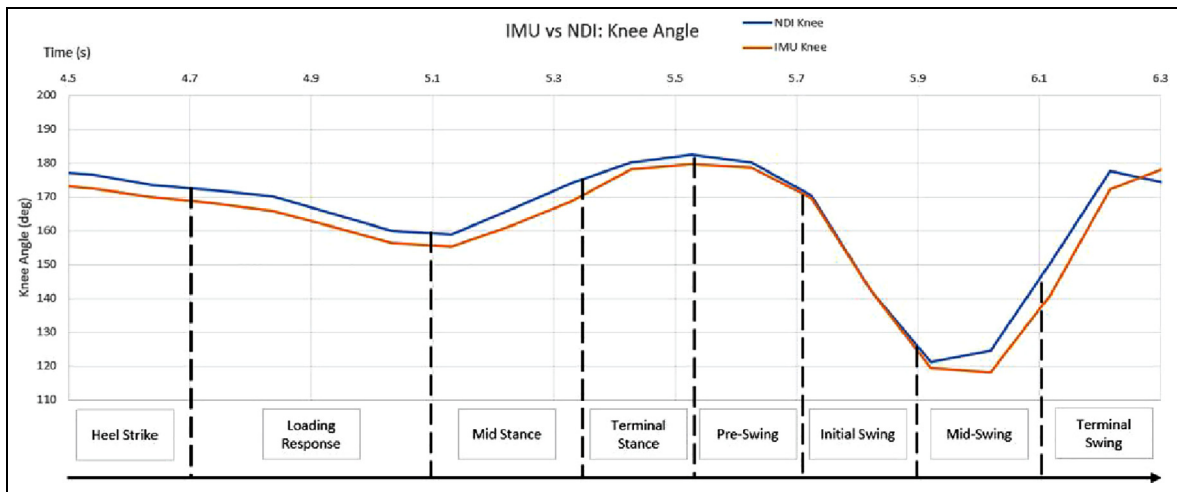

Figure 5. Gait comparison between the NDI optical tracking results and the IMU tracking results.

comparison of the angular variation between the NDI and IMU over a certain period.

This pre-processing included the following processes: first, all the collected raw data were checked and cleaned; since the NDI's sampling rate (60 Hz) was different from the IMU's sampling rate (50 Hz), it is important to adjust the sample sizes from both systems and make sure they are identical. Moreover, each system's data set was aligned according to the peaks of the calculated angles.

Results

Detailed result of one participant

The results of the gait analysis of one participant are shown in Figure 5. The blue line is the NDI data, and the orange line is the IMU data.

Overall results of 10 participants

The angular variations of the hip, knee, and ankle during walking and jogging for all 10 participants are shown in Figure 6.

A cross-correlation method was used to evaluate the difference between the results from the NDI and IMU. The R-value for walking, jogging, and lunging was 0.85, 0.80, and 0.90, respectively (Figure 7). The standard deviation between the IMU and NDI for walking, jogging, and lunging was 1.48°, 3.13°, and 3.33°. The average difference between the IMU and NDI for walking, jogging, and lunging was 1.61°, 2.22°, and 2.17°.

In addition, the Bland–Altman plots were generated for the three exercises: walking, jogging, and fencing lunge, respectively (Figure 8).

Discussion

The reason why three different types of motion were included is that they represent classic daily and sports exercises. The first two exercises (walking and jogging) aimed to test the IMU accuracy with greater emphasis on limb movement, whereas the exercise of a fencing lunge aimed to test the IMU accuracy with a greater focus on joint motion. All of these exercises were designed to assess the IMU accuracy across a wide range of exercising speeds and limb movements.
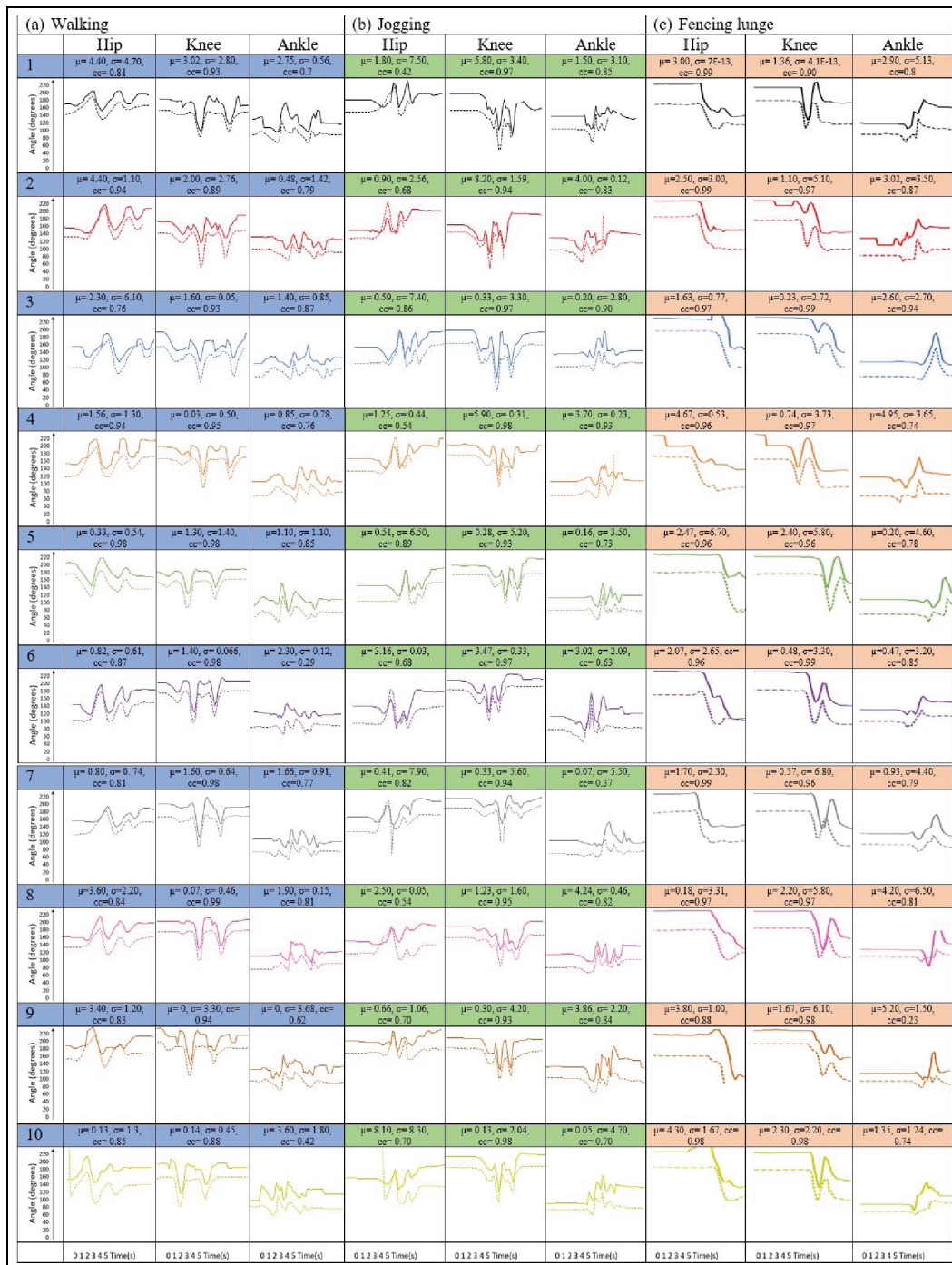
Figure 6. The walking, jogging, and fencing lunge results for 10 participants. The solid line is the IMU data, and the dashed line is the NDI data. Taking one graph of the hip movement of Subject 1 as an example, $\mu = 4.40$, $\sigma = 4.70$, and cc = 0.81 means the mean of differences is $4.40°$, the average standard deviation is $4.70°$, and the cross-correlation is 0.81. The two lines were artificially separated from each other by adding an offset of $40°$ for better presentation.

Abnormalities in the results

In Figure 6, for Subject 7, the cross-correlation was only 0.37 between the IMU and NDI ankle data. The reason was when the human participant was wearing the ankle sleeves, the tracking module moved off from the original position when he or she was jogging. This also happened when subjects were wearing smaller sizes of shoes, which gave the sleeve more room to rotate.

That explained why the cross-correlations were worse in the ankle angles.

Comparability between the NDI and the IMU

The average value for cross-correlation was 0.85. The Bland–Altman plots have also shown significant agreement between the IMU and NDI data. These findings suggest that the MEMS IMU-based angular tracking
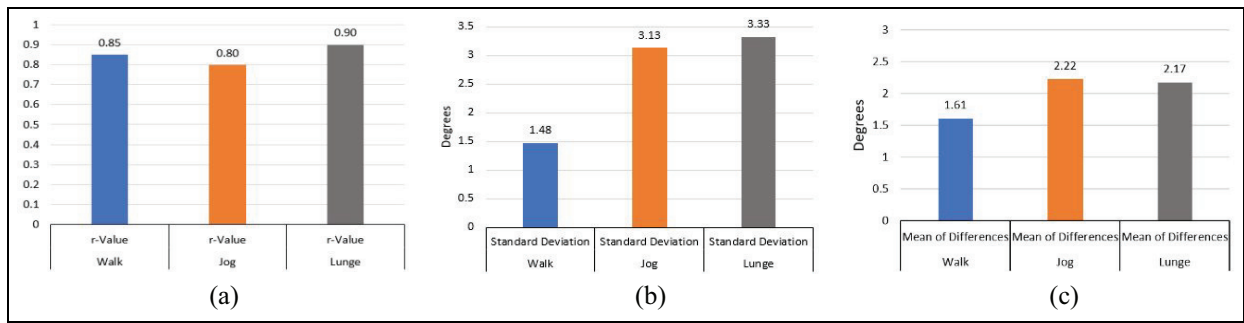
Figure 7. (a) The cross-correlation, (b) the standard deviation, and (c) the average difference for walking, jogging, and fencing lunge for 10 participants.
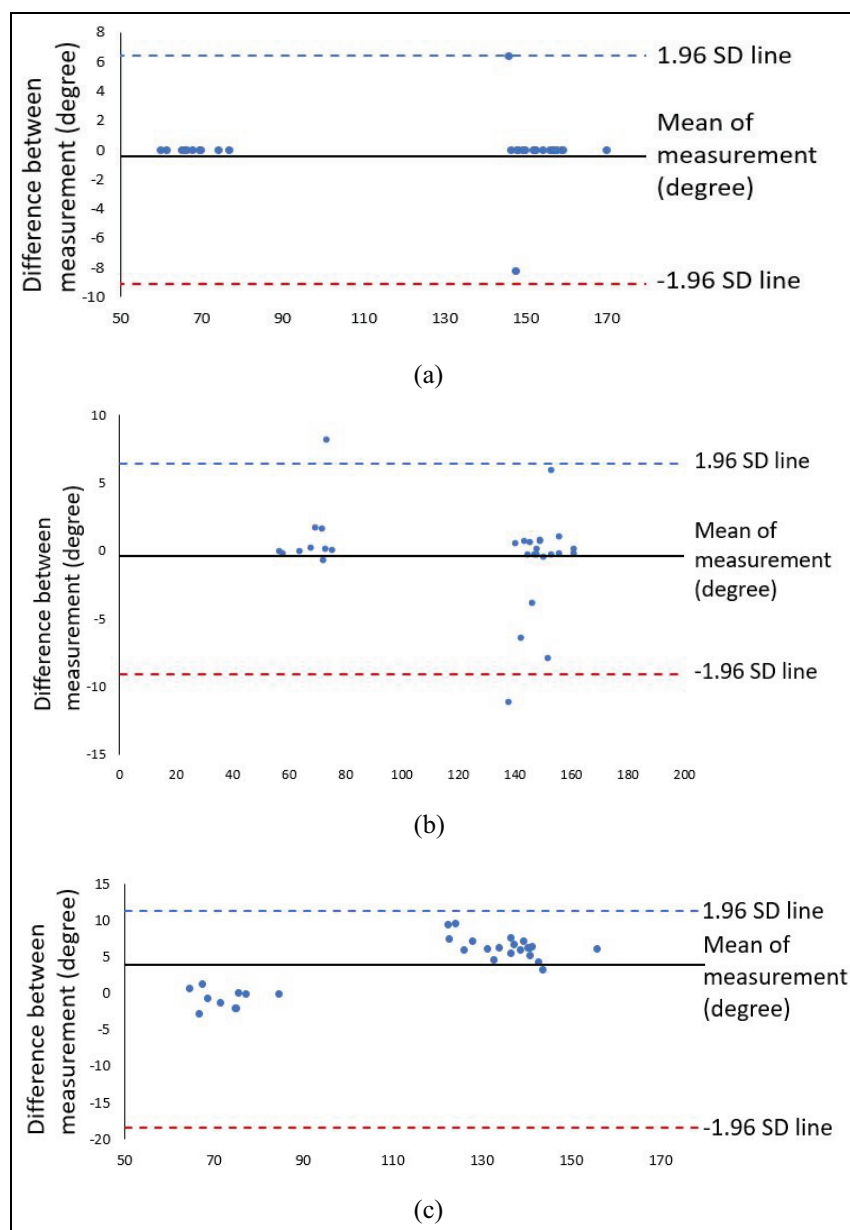

Figure 8. The Bland-Altman plots for three different exercises: (a) walking, (b) jogging, and (c) fencing lunge.

system presented in this study is comparable to a commercially available OTS. It could track real-time body motion, offering instant feedback to patients and therapists.

Limitations of NDI

The reflective markers were designed to be mounted on the side of the body (i.e. sagittal plane), specifically on the position of the iliotibial band of the thigh section, so that the reflective markers on both legs would not interfere with each other. The human subjects performed each exercise when one side of their body was exposed to the NDI, then turned around and performed the same exercise on the other side of the body. For brevity, only the results of the left side of the body were shown in Figures 3 and 4. The marker arrangement created the line-of-sight issues, such as when an arm swings down in front of the marker or a piece of clothing moves during exercise and covers the marker. This problem was solved by instructing the subjects to hold one arm above the markers when the left side of the body was facing the NDI and to tuck loose clothing into the sleeves.

Limitations of the IMU

Generally speaking, the IMU module has a drift problem on the Z-axis. To mitigate the drift problem, two solutions were used: one is to apply the Kalman filter on the Z-axis to reduce the drift and the other is to adjust the orientation of the IMU module (Figure 2(b)) so that the measured angle was derived only from the X- and Y-axis. After that, the Euler angles of the X- and Y-axis were used to calculate the tilt angle, which was ideal for measuring 2D movement. All the calculations have been conducted on a smartphone application.

Advantages of the IMU over NDI

From the experiments conducted, it can be seen that the IMU is more suitable in dynamic situations and environments than passive marker systems, such as NDI, due to the following reasons. During the experiment with the NDI, the subjects had to pay attention to the positions of markers and take actions to avoid blocking markers; this inevitably impacted the quality of exercise. In contrast, the performance of the IMU was stable and did not interfere with the body posture of the subjects. For the consideration of accurate joint angle calculation, the relative position between the optical markers has to be fixed. In this study, due to the sleeve and 3D-printed mount design, this is less problematic. However, it could be a prevalent issue in many gait analyses when the reflective markers are attached with less secure options. The IMU has its coordinate system, whereas the coordinates of NDI marker positions are dependent on the NDI emitter/receiver coordinate

system. This makes the IMU an ideal option for the fabrication of a portable movement monitoring system.

The future application of the system is to aid in training a patient to carry out the repetitive activity in an out-of-clinic environment.

Conclusion

To summarize this study, a new MEMS IMU-based angular tracking system was developed. A total of 10 human subjects were instructed to perform the three different motions: walking, running, and lunging. The same trials were then conducted together with the IMU and the NDI systems. Comparing the IMU to the NDI, the average cross-correlation value was 0.85, the standard deviation was 2.65°, and the mean difference was 2.00°. This verified that the proposed MEMS IMU-based angular tracking system is able to provide accurate information on joint angles and could potentially be used for outdoor or home-based rehabilitation.

In the future, acceleration data will be included; so more kinematic information can be integrated to generate an analysis of the repetitive rehabilitation exercise and assess the effectiveness of the exercise. Moreover, the system will detect not only the movement of the lower limbs but also the movement of the upper limbs, including the movement of the fingers, after the system is scaled down.

ORCID iDs

Rui Li https://orcid.org/0000-0003-1448-6489
Zion Tsz Ho Tse https://orcid.org/0000-0001-9741-1137

Supplemental material

Supplemental material for this article is available online.

References

1. Machida E, Cao M, Murao T, et al. Human motion tracking of mobile robot with Kinect 3D sensor. In: *Proceedings of SICE annual conference (SICE)*, Akita, Japan, 20–23 August 2012, pp.2207–2211. New York: IEEE.

2. Murray D and Basu A. Motion tracking with an active camera. *IEEE Trans Patt Anal Mach Intel* 1994; 16: 449–459.

3. Zhang J-H, Li P, Jin C-C, et al. A novel adaptive Kalman filtering approach to human motion tracking with magnetic-inertial sensors. *IEEE Trans Ind Electron*. Epub ahead of print 15 October 2019. DOI: 10.1109/TIE.2019.2946557.

4. Chang C-Y, Lange B, Zhang M, et al. Towards pervasive physical rehabilitation using Microsoft Kinect. In: *Proceedings of the 6th international conference on pervasive computing technologies for healthcare (PervasiveHealth) and workshops*, San Diego, CA, 21–24 May 2012, pp.159–162. New York: IEEE.

5. Zhao W, Reinthal MA, Espy DD, et al. Rule-based human motion tracking for rehabilitation exercises: real-time assessment, feedback, and guidance. *IEEE Access* 2017; 5: 21382–21394.

6. Hayden MR. *Huntington's chorea*. Berlin: Springer Science & Business Media, 2012.

7. Lang AE and Lozano AM. Parkinson's disease. *N Eng J Med* 1998; 339: 1130–1143.

8. Radder DL, Sturkenboom IH, van Nimwegen M, et al. Physical therapy and occupational therapy in Parkinson's disease. *Int J Neurosci* 2017; 127: 930–943.

9. Tarsy D. Treatment of Parkinson disease: a 64-year-old man with motor complications of advanced Parkinson disease. *J Am Med Assoc* 2012; 307: 2305–2314.

10. Corrales JA, Candelas F and Torres F. Hybrid tracking of human operators using IMU/UWB data fusion by a Kalman filter. In: *Proceedings of the 3rd ACM/IEEE international conference on human-robot interaction (HRI)*, Amsterdam, 12–15 March 2008, pp.193–200. New York: IEEE.

11. Yuan Q and Chen I-M. Localization and velocity tracking of human via 3 IMU sensors. *Sens Actuat A Phys* 2014; 212: 25–33.

12. Zhou H, Stone T, Hu H, et al. Use of multiple wearable inertial sensors in upper limb motion tracking. *Med Eng Phys* 2008; 30: 123–133.

13. Tian Y, Meng X, Tao D, et al. Upper limb motion tracking with the integration of IMU and Kinect. *Neurocomputing* 2015; 159: 207–218.

14. Ren H and Kazanzides P. Investigation of attitude tracking using an integrated inertial and magnetic navigation system for hand-held surgical instruments. *IEEE/ASME Trans Mechatron* 2012; 17: 210–217.

15. Guo H, Uradzinski M, Yin H, et al. Indoor positioning based on foot-mounted IMU. *Bull Polish Acad Sci Techn Sci* 2015; 63: 629–634.

16. Sun R, Aldunate RG and Sosnoff JJ. The validity of a mixed reality-based automated functional mobility assessment. *Sensors* 2019; 19: 2183.

17. Miyatake T, Lee S, Galiana I, et al. Biomechanical analysis and inertial sensing of ankle joint while stepping on an unanticipated bump. In: González-Vargas J, Ibáñez J, Contreras-Vidal J, et al. (eds) *Wearable robotics: challenges and trends*. Cham: Springer, 2017, pp.343–347.

18. Kobashi S, Tsumori Y, Imawaki S, et al. Wearable knee kinematics monitoring system of MARG sensor and pressure sensor systems. In: *IEEE international conference on system of systems engineering (SoSE)*, Albuquerque, NM, 30 May–3 June 2009, pp.1–6. New York: IEEE.

19. Müller P, Bégin M, Schauer T, et al. Alignment-free, self-calibrating elbow angles measurement using inertial sensors. *IEEE J Biomed Health Inform* 2017; 21: 312–319.

20. Mundt M, Thomsen W, David S, et al. Assessment of the measurement accuracy of inertial sensors during different tasks of daily living. *J Biomech* 2019; 84: 81–86.

21. Li R, Modlesky CM and Tse ZTH. Smartphone-enabled trackers for lower-body monitoring. In: *International symposium on medical robotics (ISMR)*, Atlanta, GA, 3–5 April 2019, pp.1–5. New York: IEEE.

22. Roush W. An Tibion's bionic leg rewire stroke victims' brains? https://xconomy.com/san-francisco/2010/12/13/can-tibions-bionic-leg-rewire-stroke-victims-brains/ (2010, accessed 3 August 2020).

23. Wiwanitkit V. Rehabilitation robotics: cost effectiveness issue. *J Rehabil Robot* 2016; 4: 1.

24. Lloréns R, Noé E, Colomer C, et al. Effectiveness, usability, and cost-benefit of a virtual reality–based telerehabilitation program for balance recovery after stroke: a randomized controlled trial. *Arch Phys Med Rehabil* 2015; 96: 418.e412–418.e425.

25. Zirbel C, Zhang X and Hughes C. The VRehab system: a low-cost mobile virtual reality system for post-stroke upper limb rehabilitation for medically underserved populations. In: *IEEE global humanitarian technology conference (GHTC)*, San Jose, CA, 18–21 October 2018, pp.1–8. New York: IEEE.

26. motion M. Optical motion capture systems, https://metamotion.com/motion-capture/optical-motion-capture-1.htm (2020, accessed 3 August 2020).

27. Morse H, Biggart L, Pomeroy V, et al. Virtual reality telerehabilitation for spatial neglect post-stroke: perspectives from stroke survivors, carers and clinicians. *medRxiv*, https://www.medrxiv.org/content/10.1101/2020.01.07.20016782v1

28. NDI. Polaris optical tracking systems, http://www.ndigital.com/medical/wp-content/uploads/sites/4/2013/12/Polaris.pdf (2013, accessed 3 August 2020).